The interpretation and measurement of the f(α) spectrum of a multifractal measure

1990 J. Phys. A: Math. Gen. 23 5295

(http://iopscience.iop.org/0305-4470/23/22/018)

J. Phys. A: Math. Gen. 23 (1990) 5295–5307. Printed in the UK

The interpretation and measurement of the $f(\alpha)$ spectrum of a multifractal measure

R C Ball and O Rath Spivack

Cavendish Laboratory, University of Cambridge, Madingley Road, Cambridge CB3 OHE, UK

Received 27 June 1990

Abstract. We analyse the growth probability distribution for diffusion limited aggregates (DLA) in terms of its $f(\alpha)$ curve, with f and α computed independently as generalized entropies, using data from 10 clusters of 10 000 to 100 000 particles. The growth probability is obtained by solving the Laplace equation numerically with a hierarchical method which improves accuracy and speed. Two additional methods are used to compare results for DLA clusters and for a few objects with simple geometry and known $f(\alpha)$ spectrum. These comparisons reinforce our results for the part of the DLA spectrum corresponding to $q \geq 0$. They also bring to light some unexpected features for $q < -0.1$, which suggest a non-universality of the scaling exponents in this region in two dimensions.

1. Introduction

Physical systems showing self-similarity have recently become the focus of much attention. Such systems arise in many areas of physics, and include strange attractors for dissipative non-linear systems (Halsey *et al* 1986a), models of turbulence (Mandelbrot 1978, Procaccia 1984), percolation clusters (de Arcangelis *et al* 1985, Rammal *et al* 1985), and kinetic aggregation clusters (Witten and Sander 1981, Jullien and Kolb 1984, Brown and Ball 1985). It has become clear that a simple description in terms of a single fractal dimension is not enough to characterize these systems and the concept of 'multifractal' has been introduced.

Given a measure defined on an object $\mathcal{C}$, the $f(\alpha)$ spectrum describes the distribution of singularities of the measure. Objects with non-trivial $f(\alpha)$ are called multifractal (Mandelbrot 1982).

$f(\alpha)$ spectra have been calculated recently for a variety of systems, including all those mentioned above. Although the interpretation of these spectra is still the subject of much current work, it is apparent that they can provide much more information than the mere fractal dimension of an object, and in particular lead to a better understanding and a rigorous characterization of the dynamical properties of such objects.

Here we calculate the $f(\alpha)$ spectrum of the growth probability distribution of diffusion limited aggregates. A new definition of f and α is introduced, which provides an interpretation of the spectrum in terms of an information dimension and also has some numerical advantages. The numerical solution of the Laplace equation is obtained by a new method which improves accuracy and speed.

0305-4470/90/225295+13$03.50

2. Theory

In order to obtain an $f(\alpha)$ spectrum we need a measure μ defined over a support $\mathcal{C}$. A typical and relevant example is the hit or growth probability distribution over a diffusion limited aggregate (DLA) (Witten and Sander 1981).

Each point $\boldsymbol{x}$ on a DLA can be assigned a probability $\mu(\boldsymbol{x})$ that growth will next occur there. The growth probability μ can be defined in many ways. Here the analogy with the dielectric breakdown model (Niemeyer *et al* 1984) is used to give

$$\mu(\boldsymbol{x}) \sim |\nabla\phi(\boldsymbol{x})| \tag{1}$$

where $\phi(\boldsymbol{x})$ is the potential field obtained by solving the Laplace equation $\Delta\phi = 0$ with boundary conditions corresponding to an equipotential cluster ($\phi = 0$) and an equipotential outer boundary ($\phi = 1$) at infinity (in practice the numerical calculations were performed using an outer boundary with a radius greater than five times the maximum dimension of the cluster along either axis).

In general the support of the measure, $\mathcal{C}$, will have some overall length-scale R and we define partitions on $\mathcal{C}$ of scale $b \leq R$ by 'coarse-graining' the space into 'boxes' of linear size b. Then each box can still be assigned a total measure μ associated with all parts of the support lying in the box.

The moments (of order q) of the probability measure are defined by

$$M_q \equiv \sum_{\text{boxes}} \mu^q = \langle \mu^{q-1} \rangle_\mu \tag{2}$$

where $\langle X \rangle_\mu$ denotes the average taken over all boxes with weighting μ, i.e. $\sum_{\text{boxes}} \mu X$, and the probability measure is normalized to 1: $\sum_{\text{boxes}} \mu = 1$. For a variety of systems (including the above DLA example) the moments have been found to obey the following scaling laws:

$$M_q \propto \left(\frac{R}{b}\right)^{-\tau(q)} \qquad \text{for } \frac{R}{b} \gg 1 \tag{3}$$

where the exponent $-\tau(q)$ is a monotonically increasing function of q. By using the Legendre transform $f(\alpha)$ of q and $\tau(q)$ (Halsey *et al* 1986b)

$$\alpha = \frac{\mathrm{d}\tau}{\mathrm{d}q} \qquad f(\alpha) = q\alpha - \tau \tag{4}$$

the scaling laws can be recast in a new form, giving, in the limit of large R/l

$$M_q \propto \int \left(\frac{R}{b}\right)^{f(\alpha)-q\alpha} \mathrm{d}\alpha \tag{5}$$

which has the simple histogram interpretation that $(R/b)^{f(\alpha)}$ boxes have probability measure $\mu = (R/b)^{-\alpha}$.

For DLA and other multifractal structures $f(\alpha)$ has been calculated both by computing the moment exponent $\tau(q)$ and also by scaling the observed distribution of μ values (see for example the review by Meakin 1988). The histogram result (5) has been widely interpreted as meaning that (in the limit of large R/b) the set of boxes with

$\mu = (R/b)^{-\alpha}$ lie on a fractal of dimension $f(\alpha)$. This interpretation is not rigorously proven, and has been qualified by Blunt (1989)

We introduce here a definition of f as an information dimension. We start from the definition

$$\tau(q) = \frac{\partial \ln M_q}{\partial X} \qquad X = \ln\left(\frac{b}{R}\right) \tag{6}$$

and apply the Legendre transform directly to yield first

$$\alpha = \frac{\mathrm{d}\tau}{\mathrm{d}q} = \frac{\partial}{\partial X}\left(\frac{\sum_{\text{boxes}} \mu^q \ln \mu}{\sum_{\text{boxes}} \mu^q}\right) \tag{7}$$

where we have assumed that $\mathrm{d}/\mathrm{d}q$ and $\sum_{\text{boxes}}$ commute. Defining for each q a new 'measure' $Q = \mu^q / \sum_{\text{boxes}} \mu^q$ we then have

$$\alpha = \frac{\partial}{\partial X}\langle \ln \mu \rangle_Q \tag{8}$$

where the average is over all boxes with weighting Q, as defined earlier. From this we can reconstruct also

$$f = \frac{\partial}{\partial X}\langle \ln Q \rangle_Q = \frac{\partial}{\partial X} \sum_{\text{boxes}} Q \ln Q \tag{9}$$

which can be formally identified as the information dimension of the 'measure' Q. The only qualification is that Q has a non-standard law of addition, in the sense that Q for a large box is not in general the sum of its values for a complete set of sub-boxes. Q is therefore not strictly a measure.

The results (8) and (9) also have immediate practical use in clarifying some known results:

(1) for $q = 1$ $Q \equiv \mu$, so $f = \alpha$;

(2) for $q = 0$ $Q =$ constant, so f is the information dimension of the support of the measure.

These results also appear to be a reasonably practical way of computing f and α at fixed q directly, without either the numerical differentiation inherent in the Legendre transform of $\tau(q)$, or the compromise of interpolating a numerical histogram.

3. Results

Values of f and α, for q in the range [-1,5], were calculated using equations (8) and (9) with data obtained from 10 different clusters. The clusters were of modest size (10 000, 30 000, 50 000 and 100 000 particles), grown on a square lattice with a (randomly selected) proportion $\epsilon = 0.414$ of second neighbour sites allowed to stick new particles as well as all first neighbour ones. This tunes out observable square lattice bias up to at least the cluster size 100 000, analogously to other studies (Barker and Ball 1990, Ball and Brady 1985).

The Laplace equation was solved numerically by iteration on the square lattice, with a new method which makes use of the successive partitions of size b later needed for the evaluation of f and α. This has proved superior to the usual iteration procedure both in terms of precision and of computer time. The number of iterations used was varied depending on the size ot the cluster in such a way as to ensure a relative error of not more than $\sim 1\%$.

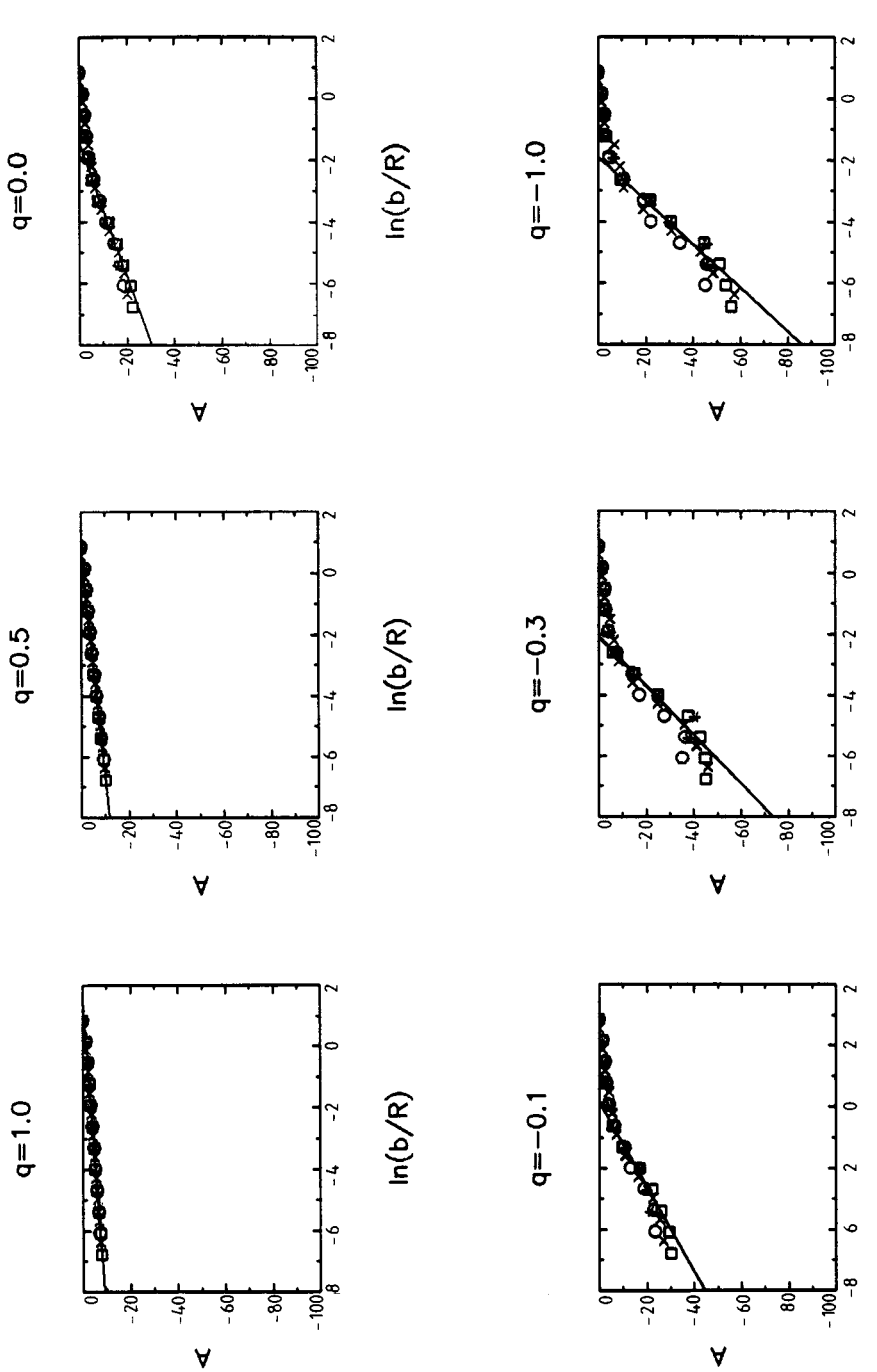

Figure 1. Typical examples of the determination of $\alpha(q)$ for three positive and three negative values of q. Here $A = \langle \ln \mu \rangle_Q$ is plotted against $\ln(b/R)$, with $R = N^{1/D}$. Only points obtained from four representative clusters are shown: *, 10 000; O, 30 000; x, 50 000; □, 10 000.

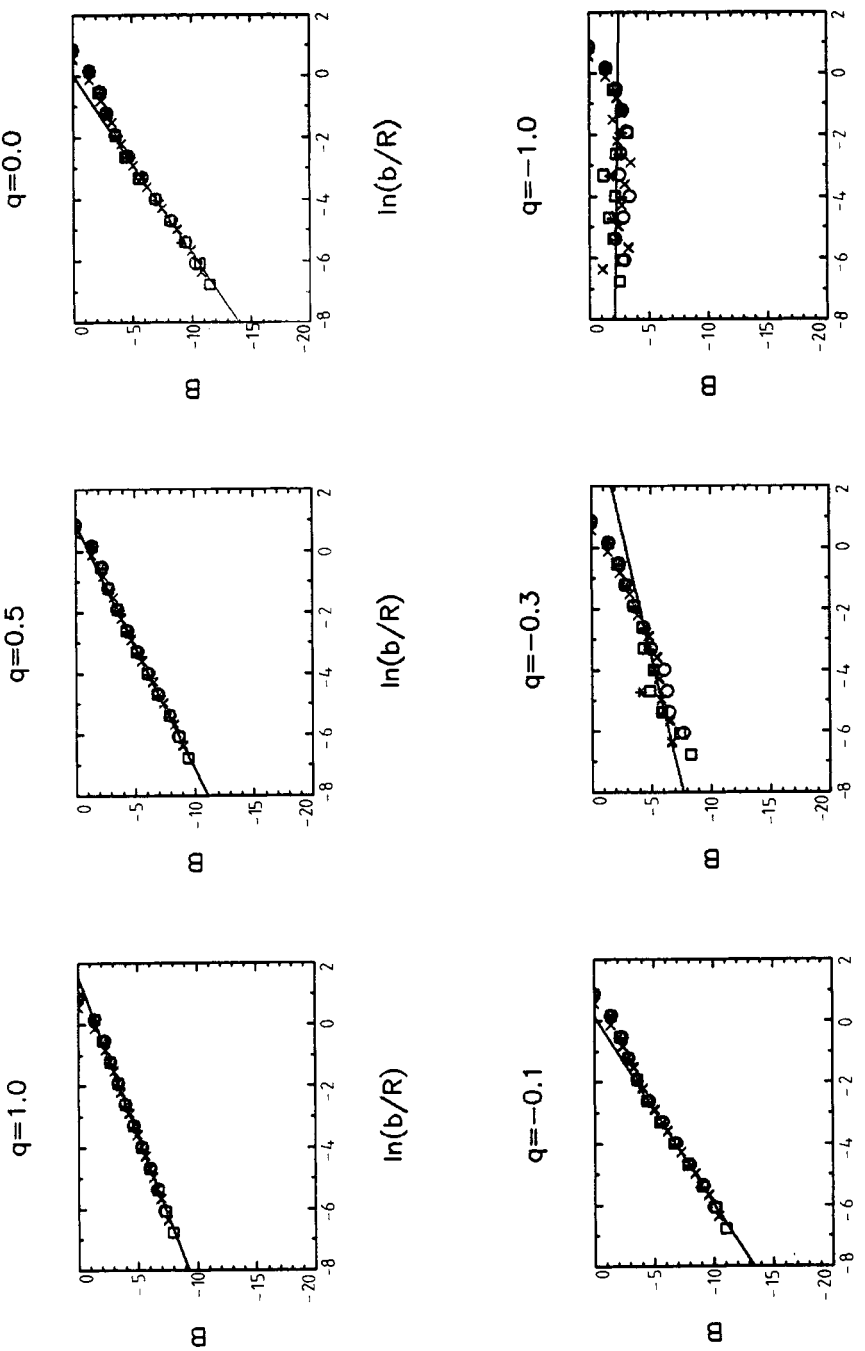

Figure 2. Typical examples of the determination of $f(q)$. Here $B = (\ln Q)_Q$ is plotted against $\ln(b/R)$, with $R = N^{1/D}$, in the same cases as in figure 1.

Figures 1 and 2 show plots of $A = \langle \ln \mu \rangle_Q$ and $B = \langle \ln Q \rangle_Q$ against $\ln(b/R)$ for these clusters: their slopes should give α and f respectively for the given q.

The box sizes b were scaled by a nominal expected cluster radius $R = N^{1/D}$, with $D = 1.70$, which gave as good a data superposition as could statistically be expected. The lack of prefactor in this choice is irrelevant to the superposition, which is also found not to be sensitive to taking a value for D elsewhere in the range 1.67 to 1.71. The radius of gyration R_G was also calculated for all clusters and the values obtained were also used to give plots of A and B against $\ln(b/R_G)$, which were compared with those obtained using the expected radius defined above. No significant difference was found. As a typical example figure 3 shows plots obtained with different choices of radii in the case $q = 0$.

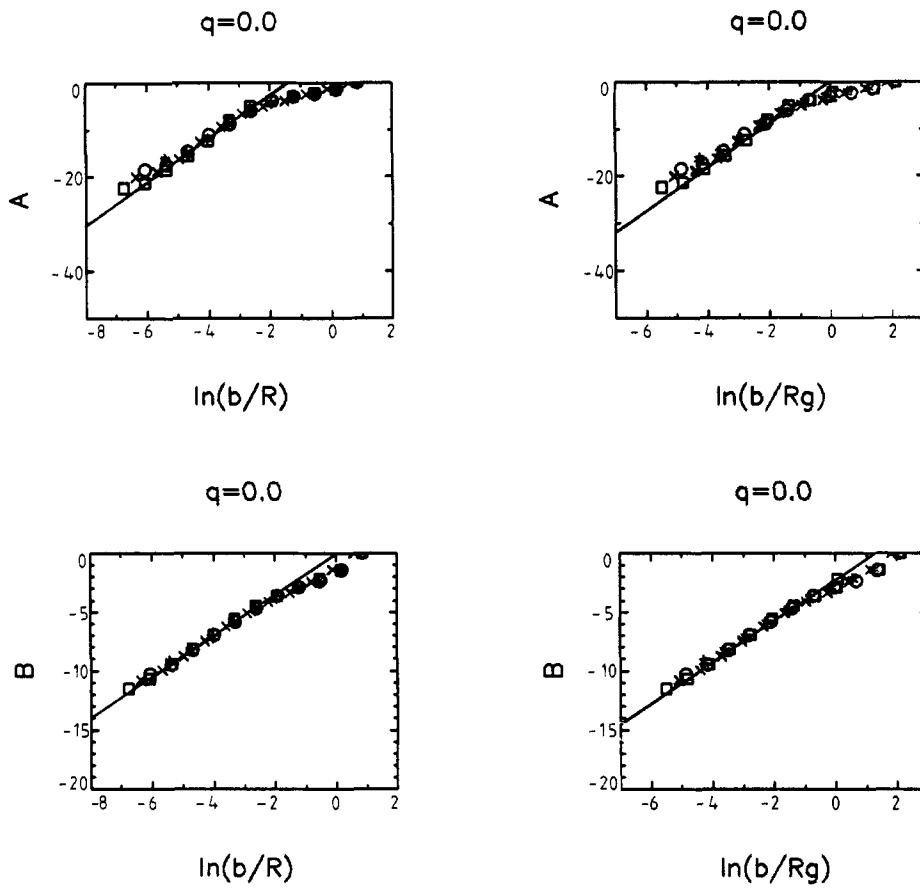

Figure 3. Graphs showing the comparison between the determination of $\alpha(q)$ and $f(q)$ from of plots of A and B against $\ln(b/R)$ when R is chosen as $R = N^{1/D}$, or as the radius of gyration $R = R_g$. In this example $q = 0$ and we use the same choice of clusters as in figures 1 and 2.

The data for A and B show, for all clusters and all $q \geq -0.1$, good scaling superposition for all but the smallest box sizes ($b = 1, 2$), with a fairly clear power law giving way to finite cluster size effects at the largest boxes. A qualification is needed with respect to the results for A with $q < 0.5$. All the plots in this range show two distinct slopes. This feature becomes more obvious as q becomes negative and larger.

One of the slopes is given by the data obtained with the first five coarsest levels of resolution (five largest boxes), and is fairly constant throughout at about 1.6 (note that this value is not far from the value of α at $q = 0.5$). The other slope is given by the remaining data, obtained with increasingly finer resolution (smaller boxes), and is different at each q. The most obvious explanation for this result stems from the observation that as q becomes more negative equation (8) is increasingly dominated by the smallest values of μ. A coarse partition (large boxes) is bound to average out small values of the probability growth. This has no effect for larger values of q, but causes all significant terms in equation (8) to be lost when q is small, thus producing a spurious constant slope.

It is well known that, since $f(\alpha)$ is dominated by small probabilities for low q, all the results obtained in this range are subject to greater numerical errors, due to the numerical errors incurred in the calculation of very small numbers. These errors are easily spotted; they lead to large uncertainties in the results, which can nevertheless be reliably quantified. The 'two-slope' behaviour described above highlights another source of error which is not so easily identified: it is indeed quite possible, if small probabilities are lost for all but the finest partition (or altogether), to obtain spurious results with very small numerical errors. This can happen very easily if only small clusters are considered.

Our measurements of the slopes were performed by least-squares fit to the regions of straight line superposition. Initially measurements were also done 'by eye' and compared with the least-squares fit to ensure reliability and eliminate spurious results. In practice this resulted in the elimination of the two points corresponding to the finest and the two points corresponding to the coarsest resolutions, for all cases with $q > 0.5$. When $q < 0.5$, four points at the coarsest resolutions had to be disregarded, due to the two-slope behaviour discussed above. We checked that the results for $q > 0.5$ were insensitive to discarding either two or four points at the coarsest resolutions. Our choice of points is designed to eliminate spurious results related to local behaviour (finest resolutions) or finite-size effects (coarsest resolutions). The values of f and α obtained are shown in table 1. In table 2 we compare our results with earlier ones, for some selected values of q. Figure 4 shows the $f(\alpha)$ curve; a few representative error bars are shown, which reflect the deviation from linearity of data obtained from different clusters and are not strictly statistical errors.

Some of the results for negative q can be improved by increasing the amount of reliable data for very small probabilities, i.e. by getting better statistics with reasonably large clusters. This is certainly feasible with the present method and should be sufficient to produce a noticeable improvement at least in the part of the $f(\alpha)$ curve where $f > 0$. Results which give $f < 0$ do not have a clear physical interpretation, given that we have not measured a large sample of clusters. Our results suggest the presence of a systematic error in the region around α_{max}: $f(\alpha)$ seems to reach a lower negative bound and then oscillate around $f(\alpha) = 0$.

Our clearest numerical result is the reinforcement of $f = D$ at $q = 0$. The corresponding value of α is higher than values reported in the literature. Previous work has given widely differing values of α_0: for example $\alpha_0 \sim 2.4$ (Amitrano *et al* 1986), $\alpha_0 = 2.97 \pm 0.04$ (Ohta and Honjo 1988), up to $\alpha_0 \sim 4.0$ (Hayakawa *et al* 1987). We find $\alpha_0 = 4.49 \pm 0.1$ and we believe that other studies simply lost precision at the top of the $f(\alpha)$ curve. Our data for positive q is corroborative; for negative q we doubt whether the earlier studies (which failed even at $q = 0$) can be greatly trusted to contribute even the first few values with any real error estimate.

Table 1. Values of $f(q)$, $\alpha(q)$ and $(q-1)D(q)$, obtained by least-squares fit to the curves $\langle \ln \mu \rangle_Q$, $\langle \ln Q \rangle_Q$ and $\ln M_q$ against $\ln(b/R)$. Data from 10 clusters of 10 000 to 100 000 are used.

q	α	f	$(q-1)D_q$
5.0	0.60 ± 0.04	0.22 ± 0.06	2.80 ± 0.06
4.0	0.62 ± 0.04	0.33 ± 0.05	2.18 ± 0.05
3.0	0.66 ± 0.04	0.47 ± 0.04	1.53 ± 0.05
2.0	0.74 ± 0.04	0.66 ± 0.03	0.83 ± 0.05
1.0	0.97 ± 0.04	0.97 ± 0.03	0.97 ± 0.03
0.5	1.40 ± 0.05	1.27 ± 0.03	-0.57 ± 0.03
0.4	1.58 ± 0.05	1.35 ± 0.03	-0.72 ± 0.03
0.3	1.87 ± 0.05	1.45 ± 0.03	-0.89 ± 0.03
0.2	2.34 ± 0.06	1.56 ± 0.03	-1.09 ± 0.03
0.15	2.70 ± 0.08	1.63 ± 0.03	-1.23 ± 0.03
0.1	3.13 ± 0.08	1.68 ± 0.03	-1.37 ± 0.03
0.05	3.72 ± 0.09	1.73 ± 0.03	-1.55 ± 0.03
0.0	4.49 ± 0.1	1.75 ± 0.04	-1.75 ± 0.04
−0.02	4.93 ± 0.2	1.74 ± 0.04	-1.84 ± 0.04
−0.04	5.37 ± 0.2	1.73 ± 0.04	-1.95 ± 0.06
−0.06	5.85 ± 0.3	1.70 ± 0.04	-2.05 ± 0.06
−0.08	6.38 ± 0.3	1.66 ± 0.06	-2.17 ± 0.08
−0.10	6.95 ± 0.4	1.61 ± 0.06	-2.31 ± 0.08
−0.14	8.19 ± 0.5	1.46 ± 0.08	-2.61 ± 0.10
−0.18	9.33 ± 0.6	1.27 ± 0.08	-2.95 ± 0.10
−0.20	9.95 ± 0.8	1.15 ± 0.10	-3.14 ± 0.20
−0.25	11.3 ± 1.0	0.85 ± 0.14	-3.68 ± 0.20
−0.30	12.2 ± 1.2	0.59 ± 0.18	-4.25 ± 0.40
−0.34	12.7 ± 1.2	0.44 ± 0.18	-4.76 ± 0.40
−0.38	13.1 ± 1.2	0.31 ± 0.20	-5.28 ± 0.50
−0.40	13.2 ± 1.2	0.26 ± 0.20	-5.54 ± 0.90
−0.45	13.4 ± 1.2	0.17 ± 0.20	-6.20 ± 0.9
−0.50	13.6 ± 1.2	0.10 ± 0.20	-6.90 ± 0.9
−0.80	13.8 ± 1.2	-0.07 ± 0.20	-10.9 ± 1.0
−1.0	13.9 ± 1.2	-0.10 ± 0.20	-13.7 ± 1.0

Table 2. Comparison between our results (a) and earlier ones, as follows: (b) Amitrano *et al* 1986; (c) Hayakawa *et al* 1987; (d) Ohta and Honjo 1988; (e) Meakin 1988; (f) Halsey *et al* 1986.

	(a)	(b)	(c)	(d)	
$\alpha(\infty)$	0.59 ± 0.04	∼0.7	0.64–0.70	0.60 ± 0.04	
$\alpha(-\infty)$	∼14.0	∼8.9	∼9.0	9.4 ± 0.02	
$\alpha(0)$	4.49 ± 0.1	∼2.4	∼4.0	2.97 ± 0.04	
$f(0)$	1.75 ± 0.04	∼1.71	1.64 ± 0.01	1.63 ± 0.01	1.713 ± 0.004[e]
D_1	0.97 ± 0.04		1.04 ± 0.01	1.13 ± 0.02	
$2D_3$	1.54 ± 0.08				1.712 ± 0.01[f]

The new method used here for the calculation of the Laplace field and of the $f(\alpha)$ spectrum has been thoroughly tested in two different ways. First we used it to calculate known $f(\alpha)$ spectra of simple non-fractal objects on a square lattice. These objects were chosen for their simplicity and in order to test different features of the spectrum separately; they are:

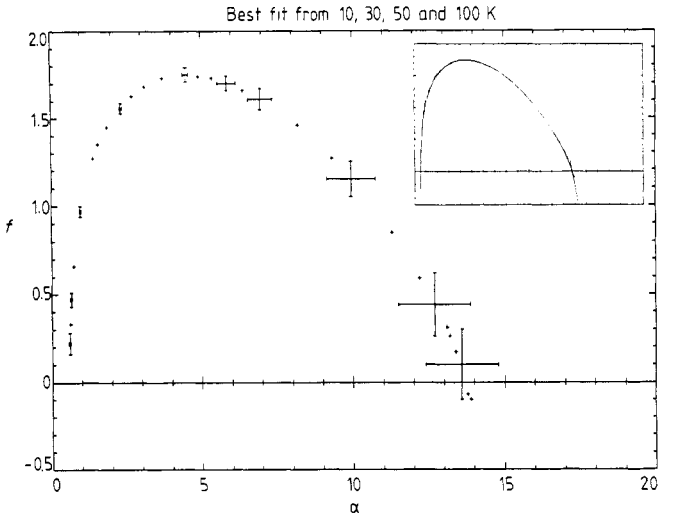

Figure 4. Graph of f against α, obtained by scaling superposition of data from 10 different clusters of sizes ranging from 10 000 to 100 000 particles. The error bars represent the standard deviation of the least-squares fit for a few representative points. The inset shows the curve obtained by drawing a segment of slope q at each point $(f(q), \alpha(q))$.

(1) a square;

(2) a concave quadrangle, in the shape of a symmetric arrow, with outer angles at the sharpest tips given by $\beta \sim 2\pi - 0.32175055$ and an angle $\gamma = \pi - 2\cos^{-1}(2/\sqrt{5}) \sim 2.2142974$ inside the single 'fjord';

(3) and (4) a circle with two equal narrow sectors removed, the two different cases corresponding to a choice of the inner angle γ given by $\gamma \simeq 0.3490659$ or $\gamma \simeq 0.2243996$, which produce $\alpha_{\max} = 9$ and $\alpha_{\max} = 14$, respectively.

The results of these tests are given in table 3 and figure 5 shows the $f(\alpha)$ spectrum

Table 3. Values of $f(q)$ and $\alpha(q)$ for the four test objects described in the text. Here the predicted values are compared with those obtained using three different methods. Method M1: $\lambda = \infty$, $\varepsilon = 1$; method M2: $\lambda = 1$, $\varepsilon = 1$; method M3: $\lambda = \infty$, $\varepsilon = 0.6$.

Object	Variable	Predicted	Method		
			M1	M2	M3
Square	$\alpha(q < 1)$	1	0.99	0.99	1.00
(723×723)	$f(q < 1)$	1	1.00	0.99	1.00
	$\alpha(q = \infty)$	2/3	0.66	0.66	0.66
Arrow	$\alpha(q = 0)$	1.0	0.99	0.99	0.99
(21 360 sites)	$f(q = 0)$	1.0	0.99	0.98	0.98
	$\alpha(q = \infty)$	0.527	0.52	0.52	0.52
	$\alpha(q = -\infty)$	1.42	1.44	1.46	1.48
Circle	$f(q = 0)$	1.0	1.06	1.06	
($\gamma \simeq 0.3490659$)	$\alpha(q = -\infty)$	9.0	9.5	9.1	
Circle	$f(q = 0)$	1.0	1.12	1.12	
($\gamma \simeq 0.2243996$)	$\alpha(q = -\infty)$	14.0	14.5	13.5	

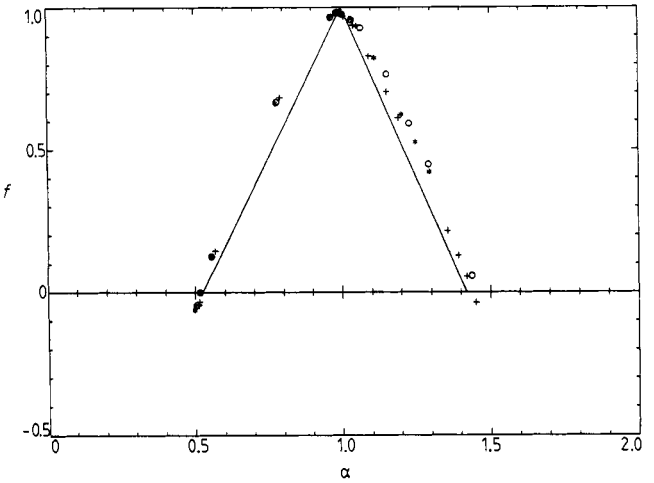

Figure 5. The $f(\alpha)$ curve for test object 2 (arrow). The exact curve is shown by the full line, and compared with results obtained with three different methods: +, $\lambda = \infty, \varepsilon = 1$ (M1); *, $\lambda = 1, \varepsilon = 1$ (M2); O, $\lambda = \infty, \varepsilon = 0.6$ (M3).

for object 2. All the results except one agree with the predicted values within 5% or better.

A second test was carried out by using different methods for the numerical solution of the Laplace equation. For this test we used a 'relaxation' method, whereby the boundary conditions on the cluster are redefined, making it absorbing (method M2), and a 'retarded relaxation' method which leaves the boundary conditions unchanged (method M3). In M2 the flux J_i on a cluster site i is given by $J_i = \overline{\phi_i} - \phi_i = \lambda\phi_i$, where $\overline{\phi_i}$ is the average of the Laplace field over nearest neighbours and λ is a parameter which we took equal to 1. In the limit $\lambda \to \infty$ this method is equivalent to the one used in section 3 (method M1). In M3 the iterative procedure leading to the value of the Laplace field on a cluster site i is defined as $\phi_i^{n+1} = \phi_i^n(1-\varepsilon) + \varepsilon\overline{\phi_i^n}$. The value $\varepsilon = 0.6$ was chosen in order to keep the computer code as simple as possible, even though it made the convergence worse and we had to increase the number of iterations in order to have results comparable to those obtained with the other methods. When $\varepsilon = 1$ this method is equivalent to M1. The correspondence between all methods is given by

$\lambda = \infty,\ \varepsilon = 1$	for method M1
$\lambda = 1,\ \varepsilon = 1$	for method M2
$\lambda = \infty,\ \varepsilon = 0.6$	for method M3.

A different value of λ involves a different renormalization, while a different value of ε involves a different relaxation of the solution, so M2 and M3 each serve as a test for different kinds of systematic errors.

We compared these methods in five cases: the four objects described above, with known $f(\alpha)$ spectrum, (see table 3) and a medium-sized (50 000 sites) DLA (see table 4). Results for the first four objects should be, in theory, exactly the same, while

Table 4. Comparison of selected results for a 50 000 sites DLA, obtained using three different methods. Method M1: $\lambda = \infty$, $\epsilon = 1$; method M2: $\lambda = 1$, $\epsilon = 1$; method M3: $\lambda = \infty$, $\epsilon = 0.6$.

	Method		
	M1	M2	M3
$f(q = 0)$	1.76	1.76	1.76
$\alpha(q = 0)$	4.73	4.26	4.72
$f(q = 1)$	0.98	1.00	0.98
$\alpha(q = \infty)$	0.59	0.58	0.59
$\alpha(q = -\infty)$	14.0	10.0	14.0
$2D_3$	1.58	1.60	1.58

for a DLA cluster there is an inherent difference deriving from our computer code, which results in completely screened sites being treated as cluster sites in method M2. In the example chosen for this test the percentage of completely screened sites is $\sim 4.2\%$ and should not affect the results.

In the part of the $f(\alpha)$ spectrum corresponding to $q \geq 0$ we found extremely good agreement between the results obtained with the three methods in all cases. When $q < 0$ there is still fairly good agreement between the results for the four test objects listed above, but this breaks down completely in the case of the DLA, where the curves obtained by methods using a different renormalization depart considerably from each other after $q = -0.1$. The main observations that can be made for the DLA can be summarized as follows.

Firstly, we note that $f(\alpha) = 1.76$ at $q = 0$ with all methods, confirming the reliability of our results at the top of the curve.

Another result we want to point out is $\alpha_{\min} \sim 0.58$. There exist theoretical predictions for the value of $\alpha_{\min}$, based on scaling arguments and on assumptions about the distribution of growth probability (Turkevich and Scher 1985). As the extremal radius R_{ext} of a cluster only increases when new growth occurs at the tips, the average rate of increase of R_{ext} is given by $(\mathrm{d}R_{\text{ext}}/\mathrm{d}N) \approx b\mu_{\text{tip}}$ (Ball and Witten 1984). From the scaling law $N \sim R^D$ and the power law dependence $\mu_{\text{tip}} \approx (b/R_{\text{ext}})^{\alpha_{\text{tip}}}$ (see equation (5)), we find $D = 1 + \alpha_{\text{tip}}$. It is generally accepted that $\alpha_{\text{tip}} = \alpha_{\min}$, i.e. the tips are the most active sites, giving the relationship $D = 1 + \alpha_{\min}$, but this is not necessarily the case (Blunt 1990). We have made checks for the occurrence of this behaviour by locating the site with maximum growth probability $\mu_{\max}$ in all the clusters included in our calculations. We found that the site with $\mu = \mu_{\max}$ almost never coincides with the extremal tip of the cluster. Therefore we have $\mu_{\text{tip}} \leq \mu_{\max}$ and the more general relationship $D \geq 1 + \alpha_{\min}$ applies.

We also find $1.58 < 2D_3 < 1.60$, i.e $2D_3 < f(0)$, which is at variance with previous predictions (Turkevich and Scher 1985, Halsey 1987). This is more difficult to explain. The linear fit for all positive values of q is particularly good, with average errors of less than 2%, and the case $q = 3$ is no exception, as can be seen in figure 6. Here, as in all other slope calculations, the first two (finest resolutions) and last two points (coarsest resolutions) are not included in the linear fit. We believe this choice eliminates local and finite-size effects, as discussed above. Nevertheless a higher value of $2D_3$ cannot be completely excluded: for comparison a line of slope 1.7 (broken line) has also been drawn on the same graph in figure 6. It should be noted, however, that the values

we obtain are always lower than predicted by the theory, for all clusters considered and whatever the method used to solve the Laplace equation, which suggests the possibility of some other source for this discrepancy, not connected with the Laplace solver. This seems to be confirmed by the structure shown on the q positive side of the $f(\alpha)$ spectra for our simple test cases (see figure 5).

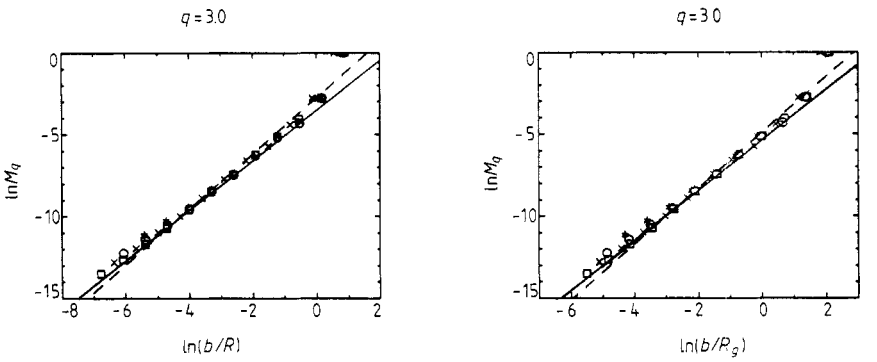

Figure 6. Determination of $\tau(q) = (q-1)D_q$, in the case $q = 3$, from plots of $\ln M_q$ against $\ln(b/R)$. Here we compare the graphs obtained with $R = N^{1/D}$ and $R = R_g$. The broken line has slope 1.7, and is shown here for comparison.

Finally, we must stress the considerable disagreement obtained for the part of the spectrum corresponding to negative values of q. As mentioned above, results from different methods diverge for $q \leq -0.1$. In particular we find $\alpha_{\max} \sim 10$ with method M2 and $\alpha_{\max} \sim 14$ with method M1 and M3, all with errors of the order of ± 1.0. All the values reported in the literature for DLA clusters are much lower: typical results are $\alpha_{\max} \sim 9$ (Hayakawa *et al* 1987), $\alpha_{\max} = 9.4 \pm 0.2$ (Ohta and Honjo 1988), $\alpha_{\max} \sim 8.9$ (Amitrano *et al* 1986). We described above our tests on objects 3 and 4, with a predicted $\alpha_{\max}$ of 9 and 14 respectively, and reported agreement for all methods.

The problem with method M2 at negative q is that it allows flux to cross arms of the cluster. As it does so only with strong screening, we originally anticipated that this would make little difference. The fact that it does has interesting implications, in that it suggests that there are backbones in the structure which separate regions of quite different measure (see also Mandelbrot 1990). This in turn raises some doubts about box-based definitions of $f(\alpha)$, which assume local spatial correlation of the measure.

The non-crossing constraint is a feature special to two dimensions, which suggest that in any search for continuous trends with dimensionality it is the M2 results which are relevant. They should also correspond, for example, to DLA growth with finite sticking probability and walkers allowed to cross cluster sites. This, of course, would imply that $f(\alpha)$ for $q < 0$ is much less universal than other scaling exponents.

4. Conclusions

We have calculated the $f(\alpha)$ spectrum of a DLA by using a good sample of medium-sized clusters, and we have tested our calculations thoroughly. Our results in the range of q positive agree very well with the literature, with the exceptions discussed above.

The discrepancy found for $2D_3$ might be connected to the relatively small size of clusters and the limitations of a square lattice. Preliminary results for a 700,000 sites cluster confirm the values obtained with smaller clusters $\alpha_{\min} \sim 0.58$ and $f(0) = 1.75$, but give $(q-1)D_q = 1.68$ at $q = 3$. This single result, though, is not statistically significant and more work is needed.

We believe our different results for $q < -0.1$ highlight a non-universality in $f(\alpha)$ in this region in two dimensions, associated with whether strict non-crossing constraints are imposed.

Two principal sources of errors affect the type of calculation carried out here. One is the necessarily finite size of the system, the other is the accuracy in the calculation of the growth probability. To some extent the errors arising from these limitations can be reduced by improving the statistics. Nevertheless, if the clusters involved are medium-sized a greater number of realizations will only improve errors for $q \geq 0$. Errors for negative values of q can only be improved by using very large clusters, and in addition are always inevitably greatly affected by numerical accuracy.

References

Amitrano C, Coniglio A and Liberto F 1986 *Phys. Rev. Lett.* **57** 1016–9

de Arcangelis L, Redner S and Coniglio A 1985 *Phys. Rev.* B **31** 4725

Ball R C and Brady R M 1985 *J. Phys. A: Math. Gen.* **18** L809–13

Ball R C and Witten T A 1984 *Phys. Rev.* A **29** 2966

Barker P W and Ball R C 1990 *Phys. Rev. Lett.* to appear

Blunt M J 1989 *Phys. Rev.* A 39 2780–2

—— 1990 private communication

Brown W D and Ball R C 1985 *J. Phys. A: Math. Gen.* **18** L517

Halsey T C, Jensen M H, Kadanoff L P, Procaccia I and Shraiman B I 1986 *Phys. Rev.* A **33** 1141–51

Halsey T C, Meakin P and Procaccia I 1986 *Phys. Rev. Lett.* **56** 854–7

Hayakawa Y, Sato S and Matsushita M 1987 *Phys. Rev.* A **36** 1963–6

Jullien R and Kolb M 1984 *J. Phys. A: Math. Gen.* **17** L639

Mandelbrot B B 1978 *Ann. Israel Phys. Soc.* **2** 225

—— 1982 *The Fractal Geometry of Nature* (San Francisco: Freeman)

—— 1990 preprint

Meakin P 1988 *Phase Transitions and Critical Phenomena* vol 12 ed C Domb and J Lebowitz p 335

Niemeyer L, Pietronero L and Wiesman H J 1984 *Phys. Rev. Lett.* **52** 1033

Ohta S and Honjo H 1988 *Phys. Rev. Lett.* **60** 611

Procaccia I 1984 *J. Stat. Phys.* **36** 649

Rammal R, Tannous C, Breton P and Tremblay A M S 1985 *Phys. Rev. Lett.* **54** 1718

Turkevich L and Scher H 1985 *Phys. Rev. Lett.* **55** 1026–9

Witten T A and Sander L M 1981 *Phys. Rev. Lett.* **47** 1400–3